Ceramics International **24** (1998) 205–209

PII: S0272-8842(97)00003-5
0272-8842/98 $19.00 + .00

A Bicontinuous Microemulsion Route to Zinc Oxide Powder

B. P. Lim, & J. Wang*
Department of Materials Science, Faculty of Science, National University of Singapore, Singapore 119260

S. C. Ng
Department of Physics, Faculty of Science, National University of Singapore, Singapore 119260

C. H. Chew & L. M. Gan
Department of Chemistry, Faculty of Science, National University of Singapore, Singapore 119260

(Received 5 November 1996; accepted 13 January 1997)

Abstract: An ultrafine zinc oxide powder of 0.15 μm in particle size has been synthesised via a microemulsion processing route, which involves preparing an inverse water-in-oil system consisting of 18.0 wt% 0.5 M $Zn(NO_3)_2$ solution as the aqueous phase, 57.4 wt% petroleum spirit (boiling point: 100–120°C) as the oil phase, and 24.6 wt% poly(oxyethylene)$_5$ nonyl phenol ether (NP5) as the non-ionic surfactant. Electrical conductivity measurement indicated that the optical transparent system exhibited a bicontinuous nanostructure. Nanosized precursor particles of zinc hydroxide were formed when an appropriate amount of 1.0 M ammonia solution was added dropwise into the bicontinuous microemulsion system. Subsequent calcination of the hydroxide precursor at 470°C for 3 h resulted in the formation of an ultrafine zinc oxide powder, which has been characterised using particle size analyser, BET specific surface area analyser, X-ray diffraction (XRD), and scanning electron microscope (SEM). © 1998 Elsevier Science Limited and Techna S.r.l.

1 INTRODUCTION

Zinc oxide and zinc oxide-based ceramic materials exhibit many unique optical and electrical/electronic properties and therefore they are being used in many demanding technological applications.[1,2] For example, zinc oxide containing a small amount of dopants such as BaO, Bi_2O_3, Sb_2O_3, CoO, and MnO_2 has been used as a low voltage varistor in many electronic devices, due to its excellent non-linear current–voltage characteristics.[3,4] Zinc oxide has also often been used as a model material in studying the densification, grain growth and microstructural development of ceramic materials.[5,6] As a low voltage varistor, its electrical and electronic properties are largely dependent on the microstructural features such as the sintering density, grain size, grain size distribution and the type and amount of dopants present in the sintered ceramic. Preparing a fine and sinterable ceramic powder of narrow particle size distribution and minimised degree of particle agglomeration is the first and perhaps the most important step in fabricating a sintered ceramic material of the desirable microstructure and therefore performance.[7–9] A variety of chemistry-based processing techniques have been used to prepare fine zinc oxide powders,[10–15] including precipitation, sol–gel, pyrolysis, hydrolysis, microwave synthesis, hydrothermal synthesis and microemulsion. The success of these processing techniques varies considerably from one to another. The aim of present work is to investigate the feasibility of producing an ultrafine zinc oxide powder via an inverse microemulsion processing route, which has been successfully used to prepare several other ceramic powder systems.[16–19]

A water-in-oil system containing a surfactant may exhibit one of the two thermodynamically

*To whom correspondence should be addressed.

stable structures:[20,21] (i) inverse microemulsion; and (ii) bicontinuous microemulsion. An inverse microemulsion is an isotropic dispersion of the aqueous droplets in the continuous oil phase. The size of the aqueous droplets is in the range of 5 to 20 nm in diameter, which is less than 1/4 wavelength of visible light. In contrast, the aqueous phase forms a continuous three-dimensional aqueous channel in the bicontinuous microemulsion. In both structures, the nanosized aqueous phase undergoes constant deformation, breakdown and coalescence. They both are optical transparent, due to the lack of substantial light scattering. Chemical reactions, such as precipitation and co-precipitation, may take place when droplets or nanosized channels containing the desirable reactants collide with each other in the inverse system. For example, the following reaction is expected to occur when a nanosized aqueous droplet or channel containing $Zn(NO_3)_2$ collides with the one containing an ammonia solution, forming zinc hydroxide:

$$Zn(NO_3)_2 + 2NH_4OH \rightarrow Zn(OH)_2 + 2NH_4NO_3 \quad (1)$$

A nanosized zinc hydroxide precursor will therefore be formed in the nanosized aqueous droplets or channels. The precursor may then be calcined at an appropriate temperature in order to prepare an ultrafine zinc oxide powder.

2 EXPERIMENTAL PROCEDURES

The starting materials for the present work included an analytical grade $Zn(NO_3)_2$ (BDH Ltd, UK), petroleum spirit (boiling point: 100–120°C, Fisons Scientific, UK), poly(oxyethylene)$_5$ nonyl phenol ether (NP5, Albright and Wilson Asia Pte Ltd, Singapore), and a 1.0 M ammonia solution (JT Baker, USA), all of which are of high purity. In establishing a phase diagram at room temperature for the ternary system consisting of 0.5 M $Zn(NO_3)_2$ aqueous solution, petroleum spirit and poly(oxyethylene)$_5$ nonyl phenol ether (NP5), the demarcation between the microemulsion region and the non-microemulsion region was worked out by systematically titrating the aqueous phase into a given oil–surfactant mixture, while clear–turbid transition was recorded. Thorough mixing of the three constituents was achieved using a Vortex mixer. A series of such demarcation points were determined by varying the oil–surfactant ratio. Since both the inverse and bicontinuous microemulsions appear optical transparent, it is impossible to differentiate the two on the basis of clear-turbid observation. As will be discussed in the following, electrical conductivity measurement indicated that the composition consisting of 18.0 wt% 0.5 M $Zn(NO_3)_2$ aqueous phase, 57.4 wt% petroleum spirit and 24.6 wt% NP5 exhibited a bicontinuous nanostructure in the microemulsion region. For the precipitation of zinc hydroxide, an appropriate amount of 1.0 M NH_4OH solution was added dropwise into the bicontinuous microemulsion while being agitated using a mechanical stirrer. The precursor was then retrieved by washing away the petroleum spirit and NP5 phases using ethanol, followed by centrifugal recovery and drying at 50°C in an electrical oven. DTA and TGA analyses were performed on the as-dried zinc hydroxide powder at a heating rate of 1°C per minute up to 900°C in air. The precursor was calcined at 470°C for 3 h in order to obtain an zinc oxide powder. Particle size analyser (Horiba LA910) and BET surface analyser (Quantachrome, Nova 2000) were used to measure the particle size distribution and specific surface area of the calcined zinc oxide powder. The calcined powder was also characterised using X-ray diffraction (XRD, Cu-Kα) and scanning electron microscope (SEM) for phase analysis and microstructural study, respectively.

3 RESULTS AND DISCUSSION

Figure 1 shows the ternary phase diagram established for the system comprising 0.5 M $Zn(NO_3)_2$ solution as the aqueous phase, petroleum spirit (boiling point: 100–120°C) as the oil phase and poly(oxyethylene)$_5$ nonylphenol ether (NP5) as the non-ionic surfactant. The microemulsion region

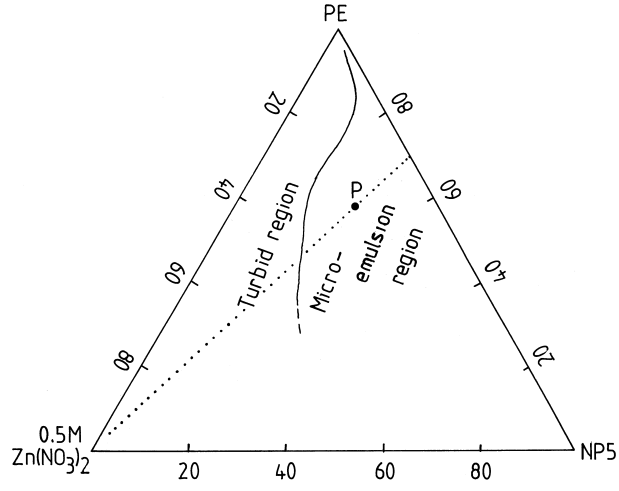

Fig. 1. The ternary phase diagram established at room temperature for the system consisting of 0.5 M $Zn(NO_3)_2$ aqueous phase, petroleum spirit (PE, boiling point: 100–120°C) and poly(oxyethylene)$_5$ nonyl phenol ether (NP5). The demarcation between the water-in-oil microemulsion and non-microemulsion regions was determined on the basis of clear–turbid observation. The compositions along the dotted line were used for conductivity measurement as shown in Fig. 2.

widens with increasing surfactant to oil phase ratio. As mentioned above, the demarcation between the transparent micromeulsion and turbid non-microemulsion regions was determined on the basis of clear–turbid observation. This, however, does not differentiate a bicontinuous microemulsion from an inverse microemulsion, as they both appear optical transparent. Therefore, electrical conductivity measurement was carried out on some selected compositions.

Figure 2 shows the electrical conductivity as a function of weight percentage of 0.5 M $Zn(NO_3)_2$ aqueous phase in the compositions along the dotted line in Fig. 1, when the oil (PE) to surfactant (NP5) ratio is fixed at 7:3. It appears that the electrical conductivity is approaching zero in the compositions containing < 5.0 wt% aqueous phase, followed by a steady increase with increasing aqueous content from 5 to 18 wt% aqueous phase where the conductivity reaches the maximum. It then decreases sharply with further increase in the aqueous content from 18 to 28 wt%. The compositions containing > 28 wt% aqueous phase exhibit an electrical conductivity of approaching zero. It may therefore be concluded, on the basis of the conductivity measurement, that a bicontinuous microemulsion is formed along the dotted line in Fig. 1 with the aqueous content ranging from 10 to 25 wt%. Further increase in the aqueous content will transform the bicontinuous nanostructure into a water-in-oil inverse microemulsion in the optical transparent region. Such a structural transformation has been observed in other microemulsion systems.[22] Therefore, the composition consisting of 18.0 wt% 0.5 M $Zn(NO_3)_2$ aqueous phase, 57.4 wt% petroleum spirit and 24.6 wt% NP5, which was chosen in the present work for the preparation of zinc oxide powder, is a bicontinuous microemulsion. It is represented by the point P in Fig. 1.

Figure 3(a) and (b) show the TGA and DTA curves, respectively, obtained at a heating rate of 10°C min^{-1} in air for the as-dried hydroxide powder, which was white in appearance. The precursor shows two falls in specimen weight with increasing heating temperature, one of which occurs over the temperature range from 140 to 190°C and the other over the temperature range from 270 to 330°C. Little weight loss was observed with increasing temperature at temperatures above 400°C, indicating the completion of all the reactions involving a weight loss. In correlating the result of TGA analysis to that of DTA study, a sharp endotherm peaking at 167.4°C was observed. Therefore, the fall in specimen weight over the temperature range from 140 to 190°C is believed to be due to the loss of residual water and organic residuals in the as-dried precursor powder. There are two apparent exotherms, peaking at 319.2 and 350.5°C, respectively.

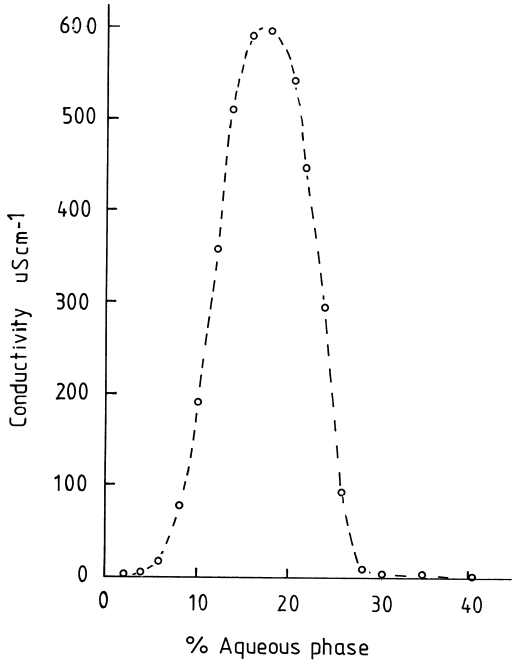

Fig. 2. The change of electrical conductivity as a function of weight percentage of 0.5 M $Zn(NO_3)_2$ aqueous phase when the oil to surfactant ratio is fixed at 7:3.

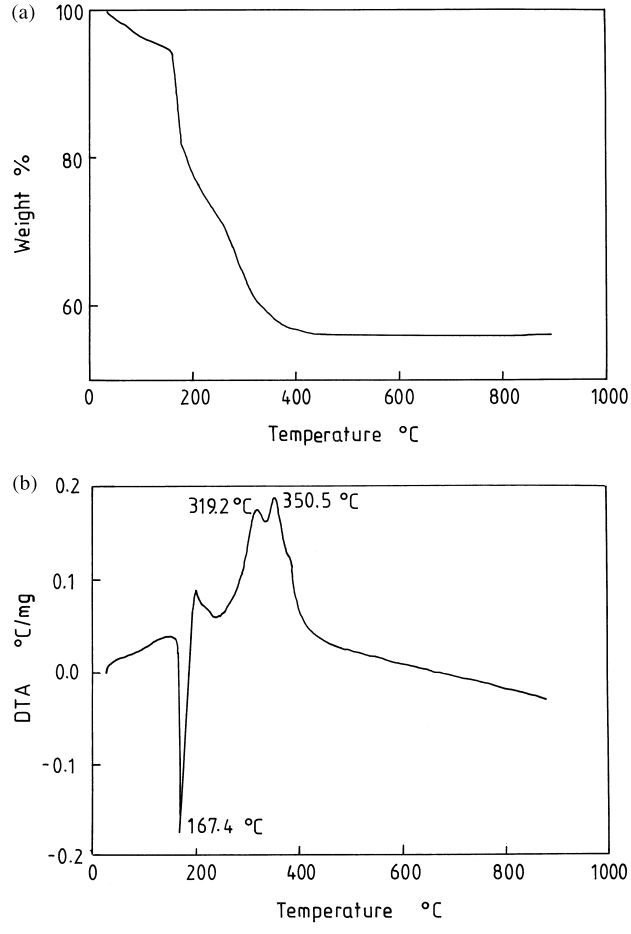

Fig. 3. The TGA (a) and DTA (b) curves obtained at a heating rate of 10°C min^{-1} in air for the as-dried hydroxide powder.

As may be expected, the hydroxide precursor undergoes decomposition with increasing temperature, forming zinc oxide which will subsequently undergo crystallisation. In many oxide ceramics, such as in zirconia and yittria, the two processes take place over almost the same temperature range.[23] Therefore, it is believed that the occurrence of the first exotherm peaking at 319.2°C is related to the decomposition of zinc hydroxide, forming zinc oxide. This is supported by the occurrence of the second fall in specimen weight over the temperature range from 270 to 330°C. The second exotherm peaking at 350.5°C is due to the subsequent crystallisation of zinc oxide, forming a crystalline oxide powder.

As shown in Fig. 3(a), little further weight loss and no any endothermic and exothermic reactions were observed with increasing heating temperature at temperatures above 400°C. Therefore, the hydroxide precursor was calcined at 470°C for 3 h in order to obtain zinc oxide powder. As shown in Fig. 4, XRD phase analysis confirms that the as-calcined powder is a high-purity crystalline zinc oxide. Figure 5 shows the particle size distribution measured using laser scattering technique for the zinc oxide powder. It consists of fine particles of sub-micrometer in sizes, with an average particle size of 0.16 μm. Its particle size distribution covers a spectrum from 0.1 to 0.8 μm. BET specific surface analysis showed that the powder exhibited a specific surface area of 6.7 $m^2 g^{-1}$, which is equivalent to an approximated average particle size of 0.15μm. Therefore, the particle sizes measured using the two techniques are in very good agreement. Figure 6 is a SEM micrograph showing that the zinc oxide powder consists of fine and nearly spherical particles of sub-micrometer in sizes. Nanosized zinc oxide crystallites are clearly visible within individual powder particles. These ultrafine crystallites are related to the nanosized hydroxide precipitate particles formed in the nanostructured bicontinuous microemulsion. Grain growth and particle agglomeration have taken place during the calcination process at 470°C

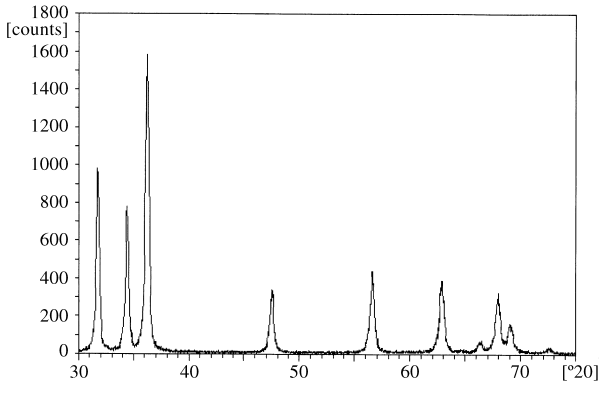

Fig. 4. XRD trace for the powder calcined at 470°C for 3 h, indicating that it is a high purity crystalline zinc oxide.

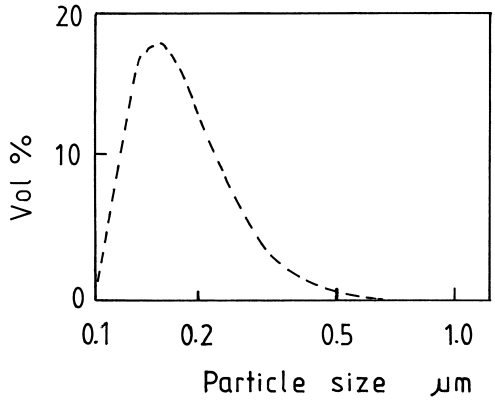

Fig. 5. The particle size distribution measured using laser scattering technique for the calcined zinc oxide powder.

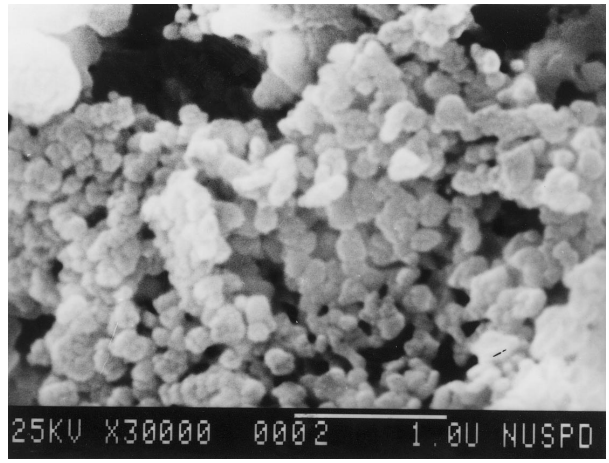

Fig. 6. An SEM micrograph showing the microstructure of the calcined zinc oxide powder.

4 SUMMARY

An ultrafine zinc oxide powder has been prepared via a microemulsion processing route. The zinc hydroxide precursor was formed by adding an appropriate amount of 1.0 M ammonia solution into a microemulsion system consisting of 18.0 wt% 0.5 M $Zn(NO_3)_2$ solution as the aqueous phase, 57.4 wt% petroleum spirit as the oil phase, and 24.6 wt% poly(oxyethylene)$_5$ nonyl phenol ether (NP5) as the non-ionic surfactant. Electrical conductivity measurement indicated that the optical transparent microemulsion system exhibited a bicontinuous nanostructure. Subsequent calcination of the bicontinuous microemulsion-derived zinc hydroxide precursor at 470°C for 3 h resulted in the formation of the ultrafine zinc oxide powder, which exhibits an approximated average particle

size of 0.15 μm, as characterised using particle size analyser and BET specific surface analyser.

ACKNOWLEDGEMENTS

The authors acknowledge the financial support provided by the National University of Singapore (Research Grant: RP950613) during the course of this investigation. B.P.L. thanks the NSTB for providing the top-up scheme.

REFERENCES

1. MOULSON, A. J. & HERBERT, J. M., *Electroceramics*. Chapman and Hall, London, 1990.
2. GUPTA, T. K., *J. Am. Ceram. Soc.,* **73** (1990) 1917.
3. LEVINSON, L. M. & PHILIPP, H. P., *Am. Ceram. Soc. Bull*., **65** (1986) 639.
4. FUJITSU, S., TOYODA, H. & YANAGIDA, H., *J. Am. Ceram. Soc*., **70** (1987) C-71.
5. SENDA, T. & BRADT, R. C., *J. Am. Ceram. Soc*., 74 (1991) 1296.
6. SHIN, S. D., SONE, C. S., HAN, J. H. & KIM, D. Y., *J. Am. Ceram. Soc*., **79** (1996) 565.
7. LANGE, F. F., *J. Am. Ceram. Soc*., **72** (1989) 3.
8. ZHENG, J. & REED, J. S., *Am. Ceram. Soc., Bull*., **71** (1992) 1410.
9. MURRAY, M. G. S., WANG, J., PONTON, C. B. & MARQUIS, P. M., *J. Mater. Sci*., **30** (1995) 3061.
10. TRINDADE, T., DEJESUS, J. D. P. & O'BRIEN, P., *J. Mater. Chem*., **4** (1994) 1611.
11. WESTIN, G., EKSTRAND, A., NYGREN, M., OSTERLUND, M., & MERKELBACH, P., *J. Mater. Chem*., **4** (1994) 615.
12. DEMERCHANT, J. & COCIVERA, M., *Chem. Mater*., **7** (1995), 1742.
13. JEZEQUE, D., GUENOT, J., JOUINI, N. & FIEVET, F., *J. Mater. Res*., **10** (1995) 77.
14. VARMA, H. K., ANANTHAKUMAR, S., WARRIER, K. G. K. & DAMODARAN, A. D., *Ceram. Int*., **22** (1996) 53.
15. ZHONG, Q. P. & MATIJEVIC, E., *J. Mat. Chem*., **6** (1996) 443.
16. GAN, L. M., CHAN, H. S. O., ZHANG, L. H., CHEW, C. H. & LOO, B. H., *Mater. Chem. Phys*., **37** (1994) 263.
17. HINGORANI, S., SHAH, D. O. & MULTANI, M. S., *J. Mater. Res*., **10** (1995) 461.
18. GAN, L. M., ZHANG, L. H., CHAN, H. S. O., CHEW, C. H. & LOO, B. H., *J. Mater. Sci*., **31** (1996) 1071.
19. LIM, G. K., WANG, J., NG, S. C. & GAN, L. M. *Mater. Lett*., **28** (1996) 431.
20. ROSANO, H. L. & CLAUSSE, M., *Microemulsion Systems*. Marcel Dekker Inc., New York, 1987.
21. MARTELLUCCI, S. & CHESTER, A. N. (ed.) *Progress in Microemulsions*. Plenum Press, New York, 1989.
22. EVANS, D. F. & WENNERSTROM, H., *The Colloidal Domain*. VCH Publishers Inc., New York, 1994, pp. 473–478.
23. WANG, J., ONG, C. L., GAN, L. M. & NG, S. C., *Mater. Lett*., **27** (1996) 239.